The **HEALPix** Primer

Prepared by: Krzysztof M. Górski, Benjamin D. Wandelt, Eric Hivon, Frode K. Hansen, and Anthony J. Banday

Abstract: **HEALPix** is a Hierarchical, Equal Area, and iso-Latitude Pixelisation of the sphere designed to support efficiently (1) local operations on the pixel set, (2) a hierarchical tree structure for multi-resolution applications, and (3) the global Fast Spherical Harmonic transform. **HEALPix** based mathematical software meets the challenges which future high resolution and large volume CMB data sets, including the WMAP and Planck mission products, will present.

TABLE OF CONTENTS

1 Introduction

The analysis of functions on domains with spherical topology occupies a central place in physical science and engineering disciplines. This is particularly apparent in the fields of astronomy, cosmology, geophysics, atomic and nuclear physics. In many cases the geometry is either dictated by the object under study or approximate spherical symmetry can be exploited to yield powerful perturbation methods. Practical limits for the purely analytical study of these problems create an urgent necessity for efficient and accurate numerical tools.

The simplicity of the spherical form belies the intricacy of global analysis on the sphere. There is no known point set which achieves the analogue of uniform sampling in Euclidean space and allows exact and invertible discrete spherical harmonic decompositions of arbitrary but band-limited functions. Any existing proposition of practical schemes for the discrete treatment of such functions on the sphere introduces some (hopefully tiny) systematic error dependent on the global properties of the point set. The goal is to minimise these errors and faithfully represent deterministic functions as well as realizations of random variates both in configuration and Fourier space while maintaining computational efficiency.

We illustrate these points using as an example the field which is particularly close to the authors' hearts, Cosmic Microwave Background (CMB) anisotropies. Here we are in the happy situation of expecting an explosion of available data within the next decade. The Microwave Anisotropy Probe (MAP) (NASA) and Planck Surveyor (ESA) missions are aiming to provide multi-frequency, high resolution, full sky measurements of the anisotropy in both temperature and polarization of the cosmic microwave background radiation. The ultimate data products of these missions — multiple microwave sky maps, each of which will have to comprise more than $\sim 10^6$ pixels in order to render the angular resolution of the instruments — will present serious challenges to those involved in the analysis and scientific exploitation of the results of both surveys.

As we have learned while working with the *COBE* mission products, the digitised sky map is an essential intermediate stage in information processing between the entry point of data acquisition by the instruments — very large time ordered data streams, and the final stage of astrophysical analysis — typically producing a 'few' numerical values of physical parameters of interest. *COBE*-DMR sky maps (angular resolution of 7° (FWHM) in three frequency bands, two channels each, 6144 pixels per map) were considered large at the time of their release.

As for future CMB maps, a whole sky CMB survey at the angular resolution of $\sim 10'$ (FWHM), discretised with a few pixels per resolution element (so that the discretisation effects on the signal are sub-dominant with respect to the effects of instrument's angular response), will require map sizes of at least $N_{pix} \sim$ a few $\times 1.5\, 10^6$ pixels. More pixels than that will be needed to represent the Planck-HFI higher resolution channels. This estimate, N_{pix}, should be multiplied by the number of frequency bands (or, indeed, by the number of individual observing channels — 74 in the case of Planck — for the analysis work to be done before the final coadded maps are made for each frequency band) to render an

approximate expected size of the already very compressed form of survey data which would be the input to the astrophysical analysis pipeline.

It appears to us that very careful attention ought to be given to devising high resolution CMB map structures which can maximally facilitate the forthcoming analyses of large size data sets, for the following reasons:

- It is clearly very easy to end up with an estimated size of many GBy for the data objects which would be directly involved in the science extraction part of the future CMB missions.

- Many essential scientific questions can only be answered by *global* studies of future data sets.

This document is an introduction to the properties of our proposed approach for a high resolution numerical representation of functions on the sphere — the Hierarchical Equal Area and iso-Latitude Pixelization (**HEALPix**, see `http://healpix.jpl.nasa.gov`), and the associated multi-purpose computer software package.

2 Discretisation of Functions on the Sphere for High Resolution Applications: a Motivation for HEALPix

Numerical analysis of functions on the sphere involves (1) a class of mathematical operations, whose objects are (2) discretised maps, i.e. quantizations of arbitrary functions according to a chosen tessellation (exhaustive partition of the sphere into finite area elements). Hereafter we mostly specialise our discussion to CMB related applications of **HEALPix**, but all our statements hold true generally for any relevant deterministic and random functions on the sphere.

Considering point (1): Standard operations of numerical analysis which one might wish to execute on the sphere include convolutions with local and global kernels, Fourier analysis with spherical harmonics and power spectrum estimation, wavelet decomposition, nearest-neighbour searches, topological analysis, including searches for extrema or zero-crossings, computing Minkowski functionals, extraction of patches and finite differencing for solving partial differential equations. Some of these operations become prohibitively slow if the sampling of functions on the sphere, and the related structure of the discrete data set, are not designed carefully.

Regarding point (2): Typically, a whole sky map rendered by a CMB experiment contains (*i*) signals coming from the sky, which are by design strongly band-width limited (in the sense of spatial Fourier decomposition) by the instrument's angular response function, and (*ii*) a projection into the elements of a discrete map, or pixels, of the observing instrument's

noise; this pixel noise should be random, and white, at least near the discretisation scale, with a band-width significantly exceeding that of all the signals.

With these considerations in mind we propose the following list of desiderata for the mathematical structure of discretised full sky maps:

1.   Hierarchical structure of the data base.   This is recognised as essential for very large data bases, and was postulated in construction of the Quadrilateralized Spherical Cube (or quad-sphere, see `http://space.gsfc.nasa.gov/astro/cobe/skymap_info.html`), which was used for the *COBE* data.   An argument in favour of this proposition states that the data elements which are nearby in a multi-dimensional configuration space (here, on the surface of a sphere), are also nearby in the tree structure of the data base, hence the near-neighbour searches are conducted optimally in the data storage medium or computer RAM. This property, especially when implemented with a small number of base resolution elements, facilitates various topological methods of analysis, and allows easy construction of wavelet transforms on quadrilateral (and also triangular) grids. Figure 1 shows how a hierarchical partition with quadrilateral structure naturally allows for a binary vector indexing of the data base.
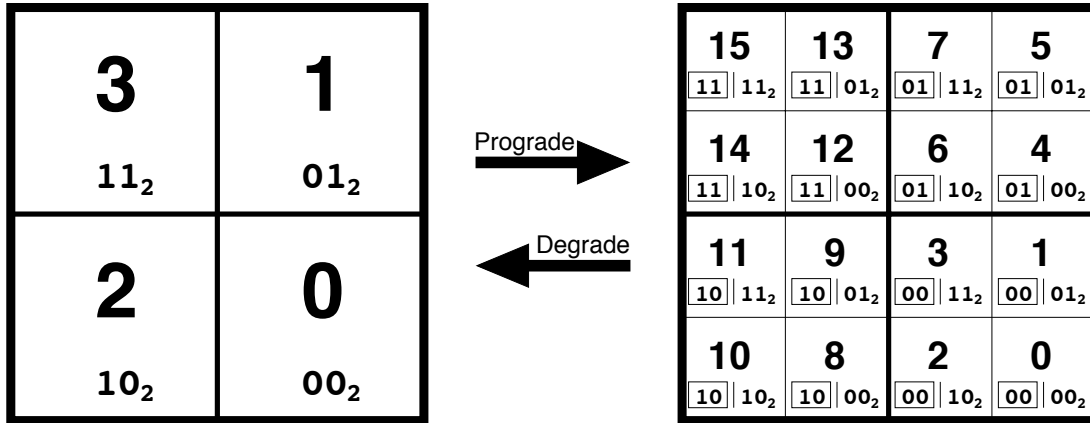

Figure 1: Quadrilateral tree pixel numbering. The coarsely pixelised coordinate patch on the left consists of four pixels. Two bits suffice to label the pixels. To increase the resolution, every pixel splits into 4 daughter pixels shown on the right. These daughters inherit the pixel index of their parent (boxed) and acquire two new bits to give the new pixel index. Several such curvilinearly mapped coordinate patches (12 in the case of **HEALPix**, and 6 in the case of the *COBE* quad-sphere) are joined at the boundaries to cover the sphere. All pixels indices carry a prefix (here omitted for clarity) which identifies which base-resolution pixel they belong to.

2. Equal areas of discrete elements of partition. This is advantageous because (*i*) white noise generated by the signal receiver gets integrated exactly into white noise in the pixel space, and (*ii*) sky signals are sampled without regional dependence, except for the dependence on pixel shapes, which is unavoidable with tessellations of the sphere.

Hence, as much as possible given the experimental details, the pixel size should be made sufficiently small compared to the instrument's resolution to avoid any excessive, and pixel shape dependent, signal smoothing.

3. Iso-Latitude distribution of discrete area elements on a sphere. This property is critical for computational speed of all operations involving evaluation of spherical harmonics. Since the associated Legendre polynomial components of spherical harmonics are evaluated via slow recursions, and can not be simply handled in an analogous way to the trigonometric Fast Fourier Transform, any deviations in the sampling grid from an iso-latitude distribution result in a prohibitive loss of computational performance with the growing number of sampling points, or increasing map resolution. It is precisely this property that the *COBE* quad-sphere is lacking, and this renders it impractical for applications to high resolution data.

A number of tessellations have been used for discretisation and analysis of functions on the sphere (for example, see (Driscoll & Healy (1994)), (Muciaccia, Natoli & Vittorio (1998)) — rectangular grids, (Baumgardner & Frederickson (1985)), (Tegmark (1996)) — icosahedral grids, (Saff & Kuijlaars (1997)), (Crittenden & Turok (1998)) — 'igloo' grids, and (Szalay & Brunner (1998)) — a triangular grid), but none satisfies simultaneously all three stated requirements.

All three requirements formulated above are satisfied by construction with the Hierarchical Equal Area, iso-Latitude Pixelisation (**HEALPix**) of the sphere, which is shown in Figure 2. A more detailed description of **HEALPix**, its motivations, and applications can be found in (Górski et al (2005)).

3   Geometric and Algebraic Properties of HEALPix

HEALPix is a genuinely curvilinear partition of the sphere into exactly equal area quadrilaterals of varying shape. The base-resolution comprises twelve pixels in three rings around the poles and equator.

The resolution of the grid is expressed by the parameter N_{side} which defines the number of divisions along the side of a base-resolution pixel that is needed to reach a desired high-resolution partition.

All pixel centers are placed on $4 \times N_{side} - 1$ rings of constant latitude, and are equidistant in azimuth (on each ring). All iso-latitude rings located between the upper and lower corners of the equatorial base-resolution pixels, the equatorial zone, are divided into the same number of pixels: $N_{eq} = 4 \times N_{side}$. The remaining rings are located within the polar cap regions and contain a varying number of pixels, increasing from ring to ring with increasing distance from the poles by one pixel within each quadrant.

Pixel boundaries are non-geodesic and take the very simple forms $\cos\theta = a \pm b \cdot \phi$ in the equatorial zone, and $\cos\theta = a + b/\phi^2$, or $\cos\theta = a + b/(\pi/2 - \phi)^2$, in the polar caps. This allows one to explicitly check by simple analytical integration the exact area equality
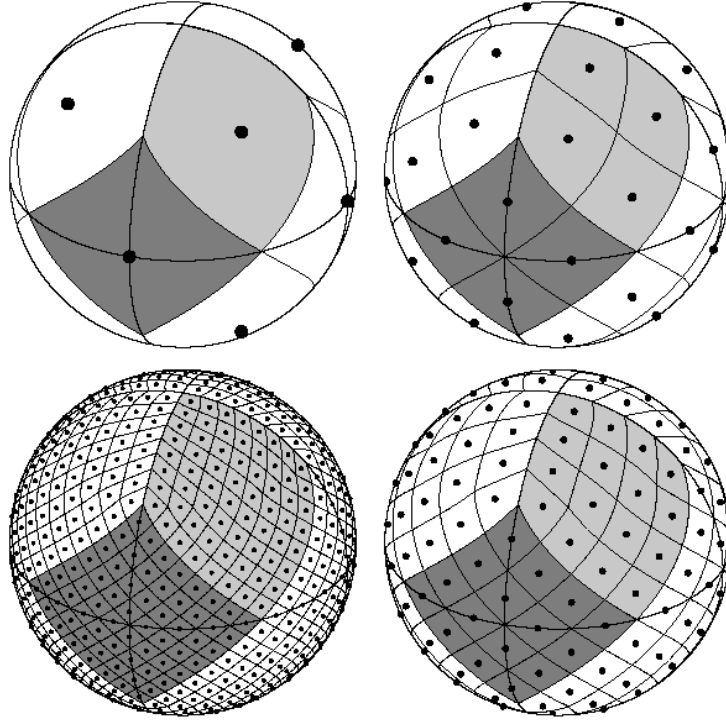
Figure 2: Orthographic view of **HEALPix** partition of the sphere. Overplot of equator and meridians illustrates the octahedral symmetry of **HEALPix**. Light-gray shading shows one of the eight (four north, and four south) identical polar base-resolution pixels. Dark-gray shading shows one of the four identical equatorial base-resolution pixels. Moving clockwise from the upper left panel the grid is hierarchically subdivided with the grid resolution parameter equal to $N_{side} = 1, 2, 4, 8$, and the total number of pixels equal to $N_{pix} = 12 \times N_{side}^2 = 12, 48, 192, 768$. All pixel centers are located on $N_{ring} = 4 \times N_{side} - 1$ rings of constant latitude. Within each panel the areas of all pixels are identical.

among pixels, and to compute efficiently more complex objects, e.g. the Fourier transforms of individual pixels.

Specific geometrical properties allow **HEALPix** to support two different numbering schemes for the pixels, as illustrated in Figure 3.

First, in the RING scheme, one can simply count the pixels moving down from the north to the south pole along each iso-latitude ring. It is in the RING scheme that Fourier transforms with spherical harmonics are easy to implement.

Second, in the NESTED scheme, one can arrange the pixel indices in twelve tree structures, corresponding to base-resolution pixels. Each of those is organised as shown in Fig. 1. This can easily be implemented since, due to the simple description of pixel boundaries, the analytical mapping of the **HEALPix** base-resolution elements (curvilinear quadrilaterals) into a [0,1]×[0,1] square exists. This tree structure allows one to implement efficiently all applications involving nearest-neighbour searches (Wandelt, Hivon & Górski (1998)), and
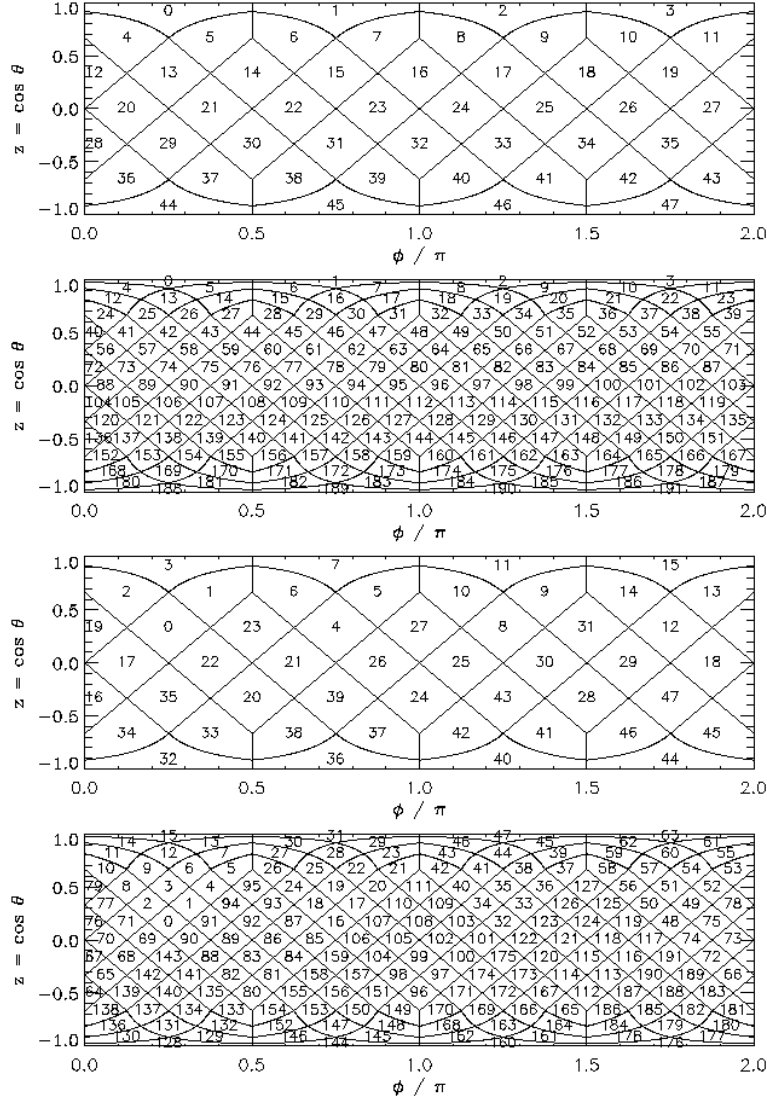
Figure 3: Cylindrical projection of the **HEALPix** division of a sphere and two natural pixel numbering schemes (RING and NESTED) allowed by **HEALPix**. Both numbering schemes map the two dimensional distribution of discrete area elements on a sphere into the one dimensional, integer pixel number array, which is essential for computations involving data sets with very large total pixel numbers. From top to bottom: Panel one (resolution parameter $N_{side} = 2$) and panel two ($N_{side} = 4$) show the RING scheme for pixel numbering, with the pixel number winding down from north to south pole through the consecutive isolatitude rings. Panel three (resolution parameter $N_{side} = 2$) and panel four ($N_{side} = 4$) show the NESTED scheme for pixel numbering within which the pixel number grows with consecutive hierarchical subdivisions on a tree structure seeded by the twelve base-resolution pixels.

also allows for an immediate construction of the fast Haar wavelet transform on **HEALPix**.

4 The HEALPix Software Package

We have developed a package of **HEALPix** based mathematical software, consisting of Fortran90 and IDL source codes as well as documentation and examples. Successful installation produces a set of facilities using standardised FITS I/O interfaces (`http://heasarc.gsfc.nasa.gov/docs/software/fitsio`) as well as two Fortran90 libraries which users can link to their own applications. Among the tasks performed by the components of the **HEALPix** package are the following:

- Simulation of the full sky CMB temperature and polarisation maps as realisations of random Gaussian fields, with an option to constrain the realisation by prior information.

- Analysis of the full sky CMB temperature and polarisation maps resulting in power spectra and/or spherical harmonic coefficients. Relevant conventions are given in Appendix A. *Note that the convention used for polarization has been changed !*.

- Global smoothing of whole sky maps with a Gaussian kernel.

- Degradation and upgrade of the resolution of discrete maps.

- Global searches on the maps for nearest-neighbours and the maxima/minima of the discretised functions.

- Algebraic conversion of the maps between the RING and NESTED numbering schemes, and mapping back and forth between positions on the sphere and discrete pixel index space.

- Pixel queries for various geometrical shapes (discs, triangles, polygons ...)

- Visualisation of the **HEALPix** formatted sky maps in the Mollweide, orthographic, cartesian cylindrical and gnomonic projections of the whole sky or small areas of it.

The package includes documents which describe the installation process, the Fortran 90 facilities, the IDL facilities and a large number of subroutines contained in the library. It is available to the scientific community at `http://healpix.jpl.nasa.gov`.

HEALPix is the format chosen by the **WMAP** collaboration to be used for the production of sky maps (see `http://map.gsfc.nasa.gov/html/technical_info.html`) from the mission data.

HEALPix software is widely used for simulation work within both the LFI and HFI consortia of the **Planck** collaboration (see `http://astro.estec.esa.nl/Planck/`).

It is also being used to analyse the data provided by the balloon CMB missions **Boomerang** (see `http://cmb.PHYS.cwru.edu/boomerang/` or `http://oberon.roma1.infn.it/boomerang/`) and **Archeops** (`http://archeops01.free.fr/main_archeops/index_english.html`).

A HEALPix conventions

A bandlimited function f on the sphere can be expanded in spherical harmonics, $Y_{\ell m}$, as

$$f(\gamma) \;\; = \;\; \sum_{\ell=0}^{l_{max}} \sum_m a_{\ell m} Y_{\ell m}(\gamma), \tag{1}$$

where γ denotes a unit vector pointing at polar angle $\theta \in [0, \pi]$ and azimuth $\phi \in [0, 2\pi)$. Here we have assumed that there is insignificant signal power in modes with $\ell > \ell_{max}$ and introduce the notation that all sums over m run from $-\ell_{max}$ to ℓ_{max} but all quantities with index ℓm vanish for $m > \ell$. Our conventions for $Y_{\ell m}$ are defined in subsection A.4 below.

Pixelising $f(\gamma)$ corresponds to sampling it at N_{pix} locations γ_p, $p \in [0, N_{\text{pix}} - 1]$. The sample function values f_p can then be used to estimate $a_{\ell m}$. A straightforward estimator is

$$\hat{a}_{\ell m} \;\; = \;\; \frac{4\pi}{N_{\text{pix}}} \sum_{p=0}^{N_{\text{pix}}-1} Y_{\ell m}^*(\gamma_p) f(\gamma_p), \tag{2}$$

where the superscript star denotes complex conjugation, and an equal weight was assumed for each pixel. This zeroth order estimator, as well as higher order estimators, are implemented in the Fortran90 facility `anafast`, included in the package. Publications discussing these estimators and the generalised quadrature problem on the sphere (Hivon *et al.*) are in preparation.

A.1 Angular power spectrum conventions

These $\hat{a}_{\ell m}$ can be used to compute estimates of the angular power spectrum $\hat{C}_\ell$ as

$$\hat{C}_\ell \;\; = \;\; \frac{1}{2l+1} \sum_m |\hat{a}_{\ell m}|^2. \tag{3}$$

The **HEALPix** package contains the Fortran90 facility `synfast` which takes as input a power spectrum C_ℓ and generates a realisation of $f(\gamma_p)$ on the **HEALPix** grid. The convention for power spectrum input into `synfast` is straightforward: each C_ℓ is just the expected variance of the $a_{\ell m}$ at that ℓ.

> **Example**: The spherical harmonic coefficient a_{00} is the integral of the $f(\gamma)/\sqrt{4\pi}$ over the sphere. To obtain realisations of functions which have a_{00} distributed as a Gaussian with zero mean and variance 1, set C_0 to 1. The value of the synthesised function at each pixel will be Gaussian distributed with mean zero and variance $1/(4\pi)$. As required, the integral of $f(\gamma)$ over the full 4π solid angle of the sphere has zero mean and variance 4π.

Note that this definition implies the standard result that the total power at the angular wavenumber ℓ is $(2l+1)C_\ell$, because there are $2\ell+1$ modes for each ℓ.

This defines unambiguously how the C_ℓ have to be defined given the units of the physical quantity f. In cosmic microwave background research, popular choices for simulated maps are

- $\Delta T/T$, a dimensionless quantity measuring relative fluctuations about the average CMB temperature.

- The absolute quantity ΔT in μK or K.

A.2   HEALPix and CMBFAST

A widely used solver of the Boltzmann equations for the computation of theoretical predictions of the spectrum of CMB anisotropy is CMBFAST (`http://www.physics.nyu.edu/matiasz/CMBFAST/cmbfast.html`).

CMBFAST makes its outputs in ASCII files, which instead of $C_{X,\ell}$ contain quantities defined as

$$D_{X,\ell} \;\; = \;\; \frac{l(l+1)}{(2\pi)T_{CMB}^2}C_{X,\ell}, \tag{4}$$

where $T_{CMB} = 2.726K$ is the temperature of the CMB today and X stands for T, E, B or C (see § A.3).

The version 4.0 of CMBFAST also created a FITS file containing the power spectra $C_{X,\ell}$, designed for interface with **HEALPix** . The spectra for polarization were renormalized to match the normalization used in **HEALPix** 1.1, which was different from the one used by CMBFAST and by **HEALPix** 1.2 (see § A.3.2 for details).

The newer version of CMBFAST (4.2, released in Feb. 2003) will generate FITS files containing $C_{X,\ell}$, with the same convention for polarization as the one used internally. It will therefore match the convention adopted by **HEALPix** in its version 1.2.

For backward compatibility, we provide an IDL code (`convert_oldhpx2cmbfast`) to change the normalization of existing FITS files created with CMBFAST 4.0. When created with the correct normalization (with CMBFAST 4.2) or set to the correct normalization (using `convert_oldhpx2cmbfast`), the FITS file will include a specific keyword (`POLNORM = CMBFAST`) in their header to identify them. The map simulation code `synfast` will issue a warning if the input power spectrum file does not contain the keyword `POLNORM`, but no attempt will be made to renormalize the power spectrum. If the keyword is present, it will be inherited by the simulated map.
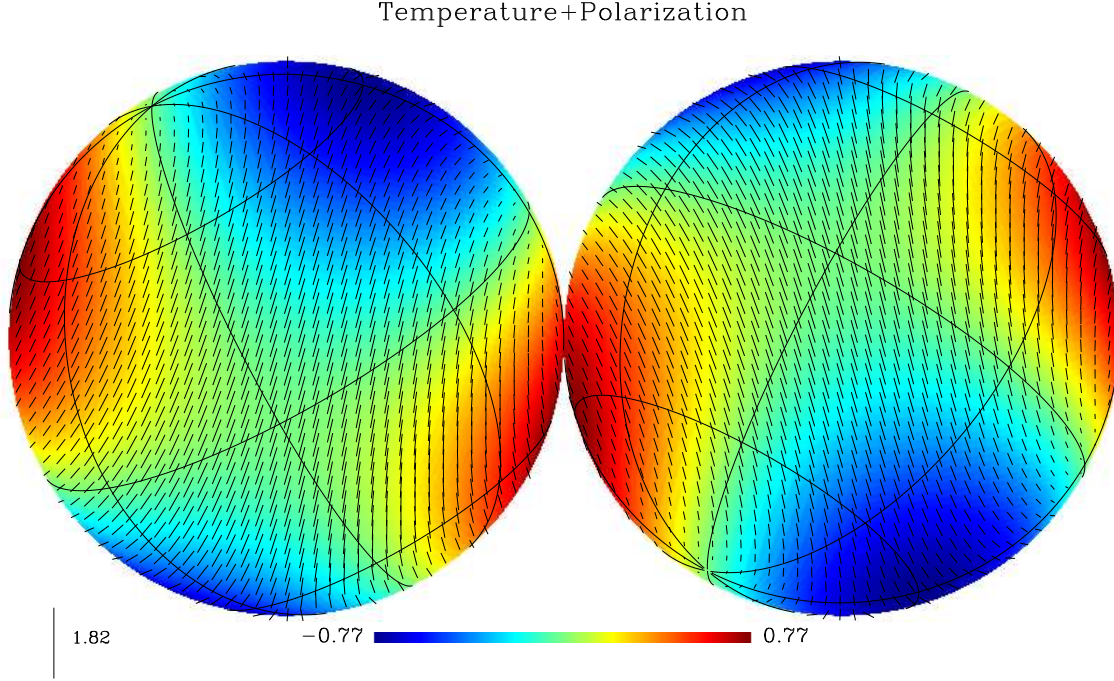
Figure 4: Orthographic projection of a fake full sky for temperature (color coded) and polarization (represented by the rods). All the input Spherical Harmonics coefficients are set to 0, except for $a_{21}^{TEMP} = -a_{2-1}^{TEMP} = 1$ and $a_{21}^{GRAD} = -a_{2-1}^{GRAD} = 1$

A.3 Polarisation convention

A.3.1 Internal convention

Starting with version 1.20 (released in Feb 2003),**HEALPix** uses the same conventions as CMBFAST for the sign and normalization of the polarization power spectra, as exposed below (adapted from (Zaldarriaga (1998))). How this relates to what was used in previous releases is exposed in A.3.2.

The CMB radiation field is described by a 2×2 intensity tensor I_{ij} (Chandrasekhar (1960)). The Stokes parameters Q and U are defined as $Q = (I_{11} - I_{22})/4$ and $U = I_{12}/2$, while the temperature anisotropy is given by $T = (I_{11} + I_{22})/4$. The fourth Stokes parameter V that describes circular polarization is not necessary in standard cosmological models because it cannot be generated through the process of Thomson scattering. While the temperature is a scalar quantity Q and U are not. They depend on the direction of observation $\mathbf{n}$ and on the two axis $(\mathbf{e_1}, \mathbf{e_2})$ perpendicular to $\mathbf{n}$ used to define them. If for a given $\mathbf{n}$ the axes $(\mathbf{e_1}, \mathbf{e_2})$ are rotated by an angle ψ such that $\mathbf{e_1}' = \cos\psi \, \mathbf{e_1} + \sin\psi \, \mathbf{e_2}$ and $\mathbf{e_2}' = -\sin\psi \, \mathbf{e_1} + \cos\psi \, \mathbf{e_2}$ the Stokes parameters change as

$$
\begin{aligned}
Q' &= \cos 2\psi \, Q + \sin 2\psi \, U \\
U' &= -\sin 2\psi \, Q + \cos 2\psi \, U
\end{aligned}
\tag{5}
$$

To analyze the CMB temperature on the sky, it is natural to expand it in spherical harmonics. These are not appropriate for polarization, because the two combinations $Q \pm iU$ are quantities of spin ± 2 (Goldberg (1967)). They should be expanded in spin-weighted harmonics $_{\pm 2}Y_l^m$ (Zaldarriaga & Seljak (1997)), (Seljak & Zaldarriaga (1997)),

$$
\begin{array}{rcl}
T(\mathbf{n}) & = & \sum_{lm} a_{T,lm} Y_{lm}(\mathbf{n}) \\
(Q + iU)(\mathbf{n}) & = & \sum_{lm} a_{2,lm}\, _2Y_{lm}(\mathbf{n}) \\
(Q - iU)(\mathbf{n}) & = & \sum_{lm} a_{-2,lm}\, _{-2}Y_{lm}(\mathbf{n}).
\end{array} \tag{6}
$$

To perform this expansion, Q and U in equation (6) are measured relative to $(\mathbf{e_1}, \mathbf{e_2}) = (\mathbf{e}_\theta, \mathbf{e}_\phi)$, the unit vectors of the spherical coordinate system. Where $\mathbf{e}_\theta$ is tangent to the local meridian and directed from North to South, and $\mathbf{e}_\phi$ is tangent to the local parallel, and directed from West to East. The coefficients $_{\pm 2}a_{lm}$ are observable on the sky and their power spectra can be predicted for different cosmological models. Instead of $_{\pm 2}a_{lm}$ it is convenient to use their linear combinations

$$
\begin{array}{rcl}
a_{E,lm} & = & -(a_{2,lm} + a_{-2,lm})/2 \\
a_{B,lm} & = & -(a_{2,lm} - a_{-2,lm})/2i,
\end{array} \tag{7}
$$

which transform differently under parity. Four power spectra are needed to characterize fluctuations in a gaussian theory, the autocorrelation between T, E and B and the cross correlation of E and T. Because of parity considerations the cross-correlations between B and the other quantities vanish and one is left with

$$
\langle a^*_{X,lm} a_{X,lm'} \rangle = \delta_{m,m'} C_{Xl} \quad \langle a^*_{T,lm} a_{E,lm} \rangle = \delta_{m,m'} C_{Cl}, \tag{8}
$$

where X stands for T, E or B, $\langle \cdots \rangle$ means ensemble average and $\delta_{i,j}$ is the Kronecker delta.

We can rewrite equation (6) as

$$
\begin{array}{rcl}
T(\mathbf{n}) & = & \sum_{lm} a_{T,lm} Y_{lm}(\mathbf{n}) \\
Q(\mathbf{n}) & = & -\sum_{lm} a_{E,lm} X_{1,lm} + i a_{B,lm} X_{2,lm} \\
U(\mathbf{n}) & = & -\sum_{lm} a_{B,lm} X_{1,lm} - i a_{E,lm} X_{2,lm}
\end{array} \tag{9}
$$

where we have introduced $X_{1,lm}(\mathbf{n}) = (\, _2Y_{lm} + \, _{-2}Y_{lm})/2$ and $X_{2,lm}(\mathbf{n}) = (\, _2Y_{lm} - \, _{-2}Y_{lm})/2$. They satisfy $Y^*_{lm} = (-1)^m Y_{l-m}$, $X^*_{1,lm} = (-1)^m X_{1,l-m}$ and $X^*_{2,lm} = (-1)^{m+1} X_{2,l-m}$ which together with $a_{T,lm} = (-1)^m a^*_{T,l-m}$, $a_{E,lm} = (-1)^m a^*_{E,l-m}$ and $a_{B,lm} = (-1)^m a^*_{B,l-m}$ make T, Q and U real.

In fact $X_{1,lm}(\mathbf{n})$ and $X_{2,lm}(\mathbf{n})$ have the form, $X_{1,lm}(\mathbf{n}) = \sqrt{(2l+1)/4\pi} F_{1,lm}(\theta)\, e^{im\phi}$ and $X_{2,lm}(\mathbf{n}) = \sqrt{(2l+1)/4\pi} F_{2,lm}(\theta)\, e^{im\phi}$, $F_{(1,2),lm}(\theta)$ can be calculated in terms of Legendre polynomials (Kamionkowski et al (1997))

$$
\begin{array}{rcl}
F_{1,lm}(\theta) & = & N_{lm} \left[-\left(\dfrac{l - m^2}{\sin^2 \theta} + \dfrac{1}{2} l(l-1) \right) P_l^m(\cos \theta) + (l+m) \dfrac{\cos \theta}{\sin^2 \theta} P_{l-1}^m(\cos \theta) \right] \\
F_{2,lm}(\theta) & = & N_{lm} \dfrac{m}{\sin^2 \theta} [-(l-1)\cos \theta P_l^m(\cos \theta) + (l+m) P_{l-1}^m(\cos \theta)],
\end{array} \tag{10}
$$

where

$$N_{lm}(\theta) \;\;=\;\; 2\sqrt{\frac{(l-2)!(l-m)!}{(l+2)!(l+m)!}}. \tag{11}$$

Note that $F_{2,lm}(\theta) = 0$ if $m = 0$, as it must to make the Stokes parameters real.

The correlation functions between 2 points on the sky (noted 1 and 2) separated by an angle β can be calculated using equations (8) and (9). However, as pointed out in (Kamionkowski et al (1997)), the natural coordinate system to express the correlations is one in which $\mathbf{e_1}$ vectors at each point are tangent to the great circle connecting these 2 points, with the $\mathbf{e_2}$ vectors being perpendicular to the $\mathbf{e_1}$ vectors. With this choice of reference frames, and using the addition theorem for the spin harmonics (Hu & White (1997)),

$$\sum_m {}_{s_1}Y_{lm}^*(\mathbf{n_1})\; {}_{s_2}Y_{lm}(\mathbf{n_2}) \;\;=\;\; \sqrt{\frac{2l+1}{4\pi}}\; {}_{s_2}Y_{l-s_1}(\beta,\psi_1)e^{-is_2\psi_2} \tag{12}$$

we have (Kamionkowski et al (1997))

$$\langle T_1 T_2 \rangle \;\;=\;\; \sum_l \frac{2l+1}{4\pi} C_{Tl} P_l(\cos\beta)$$

$$\langle Q_r(1)Q_r(2) \rangle \;\;=\;\; \sum_l \frac{2l+1}{4\pi} [C_{El} F_{1,l2}(\beta) - C_{Bl} F_{2,l2}(\beta)]$$

$$\langle U_r(1)U_r(2) \rangle \;\;=\;\; \sum_l \frac{2l+1}{4\pi} [C_{Bl} F_{1,l2}(\beta) - C_{El} F_{2,l2}(\beta)]$$

$$\langle T(1)Q_r(2) \rangle \;\;=\;\; -\sum_l \frac{2l+1}{4\pi} C_{Cl} F_{1,l0}(\beta)$$

$$\langle T(1)U_r(2) \rangle \;\;=\;\; 0. \tag{13}$$

The subscript r here indicate that the Stokes parameters are measured in this particular coordinate system. We can use the transformation laws in equation (5) to write (Q,U) in terms of (Q_r, U_r).

The definitions above imply that the variances of the temperature and polarization are related to the power spectra by

$$\langle TT \rangle \;\;=\;\; \sum_l \frac{2l+1}{4\pi} C_{Tl}$$

$$\langle QQ \rangle + \langle UU \rangle \;\;=\;\; \sum_l \frac{2l+1}{4\pi}(C_{El} + C_{Bl})$$

$$\langle TQ \rangle = \langle TU \rangle \;\;=\;\; 0. \tag{14}$$

It is also worth noting that with these conventions, the cross power C_{Cl} for scalar perturbations must be positive at low ℓ, in order to produce *at large scales* a radial pattern of polarization around cold temperature spots (and a tangential pattern around hot spots) as it is expected from scalar perturbations (Crittenden et al (1995)).

Note that Eq. (9) implies that, if the Stokes parameters are rotated *everywhere* via

$$\left(\begin{array}{c} Q' \\ U' \end{array} \right) = \left(\begin{array}{cc} \cos 2\psi & \sin 2\psi \\ -\sin 2\psi & \cos 2\psi \end{array} \right) \left(\begin{array}{c} Q \\ U \end{array} \right), \tag{15}$$

then the polarized a_{lm} coefficients are submittted to the same rotation

$$\left(\begin{array}{c} a'_{E,lm} \\ a'_{B,lm} \end{array} \right) = \left(\begin{array}{cc} \cos 2\psi & \sin 2\psi \\ -\sin 2\psi & \cos 2\psi \end{array} \right) \left(\begin{array}{c} a_{E,lm} \\ a_{B,lm} \end{array} \right). \tag{16}$$

Finally, with these conventions, a polarization with $(Q > 0, U = 0)$ will be along the North–South axis, and $(Q = 0, U > 0)$ will be along a North-West to South-East axis (see Fig. 5)

A.3.2   Relation to previous releases

Even though it was stated otherwise in the documention, **HEALPix** used a different convention for the polarization in its previous releases. The tensor harmonics approach ((Kamionkowski et al (1997)), hereafter KKS) was used, instead of the current spin weighted spherical harmonics. These two approaches differ by the normalisation and sign of the basis functions used, which in turns change the normalisation of the power spectra. Table 1 summarize the relations between the CMB power spectra in the different releases. See § A.2 about the interface between **HEALPix** and CMBFAST.

Table 1: Relation between CMB power spectra conventions used in HEALPix, CMBFAST and KKS. The power spectra on the same row are equal.

Component	**HEALPix** $\geq 1.2^a$	CMBFAST	KKS	**HEALPix** $\leq 1.1^b$
Temperature	C_ℓ^{TEMP}	$C_{\text{T},\ell}$	C_ℓ^{T}	C_ℓ^{TEMP}
Electric or Gradient	C_ℓ^{GRAD}	$C_{\text{E},\ell}$	$2C_\ell^{\text{G}}$	$2C_\ell^{\text{GRAD}}$
Magnetic or Curl	C_ℓ^{CURL}	$C_{\text{B},\ell}$	$2C_\ell^{\text{C}}$	$2C_\ell^{\text{CURL}}$
Temp.-Electric cross correlation	$C_\ell^{\text{T}-\text{GRAD}}$	$C_{\text{C},\ell}$	$-\sqrt{2}\,C_\ell^{\text{TG}}$	$\sqrt{2}C_\ell^{\text{T}-\text{GRAD}}$

[a]Version 1.2 (Feb 2003) or more recent of **HEALPix** package
[b]Version 1.1 or older of **HEALPix** package

Introducing the matrices

$$M_{\ell m} = \left(\begin{array}{cc} X_{1,\ell m} & iX_{2,\ell m} \\ -iX_{2,\ell m} & X_{1,\ell m} \end{array} \right) \tag{17}$$

where the basis functions X_1 and X_2 have been defined in Eqs. (10) and above, the decomposition in spherical harmonics coefficients (9) of a given map of the Stokes parameter Q

and U can be written in the case of **HEALPix** 1.2 as

$$\begin{pmatrix} Q \\ U \end{pmatrix} = \sum_{\ell m} M_{\ell m} \begin{pmatrix} -a_{\ell m}^{\mathrm{GRAD}} \\ -a_{\ell m}^{\mathrm{CURL}} \end{pmatrix}. \tag{18}$$

For KKS, with the same definition of M, the decomposition reads

$$\begin{pmatrix} Q \\ -U \end{pmatrix} = \sum_{\ell m} M_{\ell m} \begin{pmatrix} \sqrt{2}a_{\mathrm{E},\ell m} \\ \sqrt{2}a_{\mathrm{B},\ell m} \end{pmatrix} \tag{19}$$

whereas in **HEALPix** 1.1 it was

$$\begin{pmatrix} Q \\ U \end{pmatrix} = \sum_{\ell m} M_{\ell m} \begin{pmatrix} -\sqrt{2}a_{\ell m}^{\mathrm{GRAD}} \\ \sqrt{2}a_{\ell m}^{\mathrm{CURL}} \end{pmatrix}. \tag{20}$$

The difference between KKS and 1.1 was due to an error of sign on one the basis functions.

A.3.3   Relation with IAU convention

In a cartesian referential with axes x and y, the Stokes parameters for linear polarisation are defined such that $+Q$ is aligned with $+x$, $-Q$ with $+y$ and $+U$ with the bisectrix of $+x$ and $+y$. Although this definition is universally accepted, some confusion may still arise from the relation of this local cartesian system to the global spherical one, as described below (Hamaker & Leahy, 2003), and as illustrated in Fig. 5.

The polarization conventions defined by the International Astronomical Union (IAU, 1974) are summarized in (Hamaker & Bregman, 1996). They define at each point on the celestial sphere a cartesian referential with the x and y axes pointing respectively toward the North and East, and the z axis along the line of sight pointing toward the observer (ie, inwards) for a right-handed system.

On the other hand, following the mathematical and CMB litterature tradition, **HEALPix** defines a cartesian referential with the x and y axes pointing respectively toward the *South* and East, and the z axis along the line of sight pointing away from the observer (ie, *outwards*) for a right-handed system. The *Planck* CMB mission follows the same convention (Ansari et al, 2003).

The consequence of this definition discrepency is a change of sign of U, which, if not accounted for, jeopardizes the calculation of the Electric and Magnetic CMB polarisation power spectra.

How HEALPix deals with these discrepancies
The FITS keyword `POLCCONV` has been introduced in **HEALPix** 2.0 to describe the polarisation coordinate convention applied to the data contained in the file. Its value is either
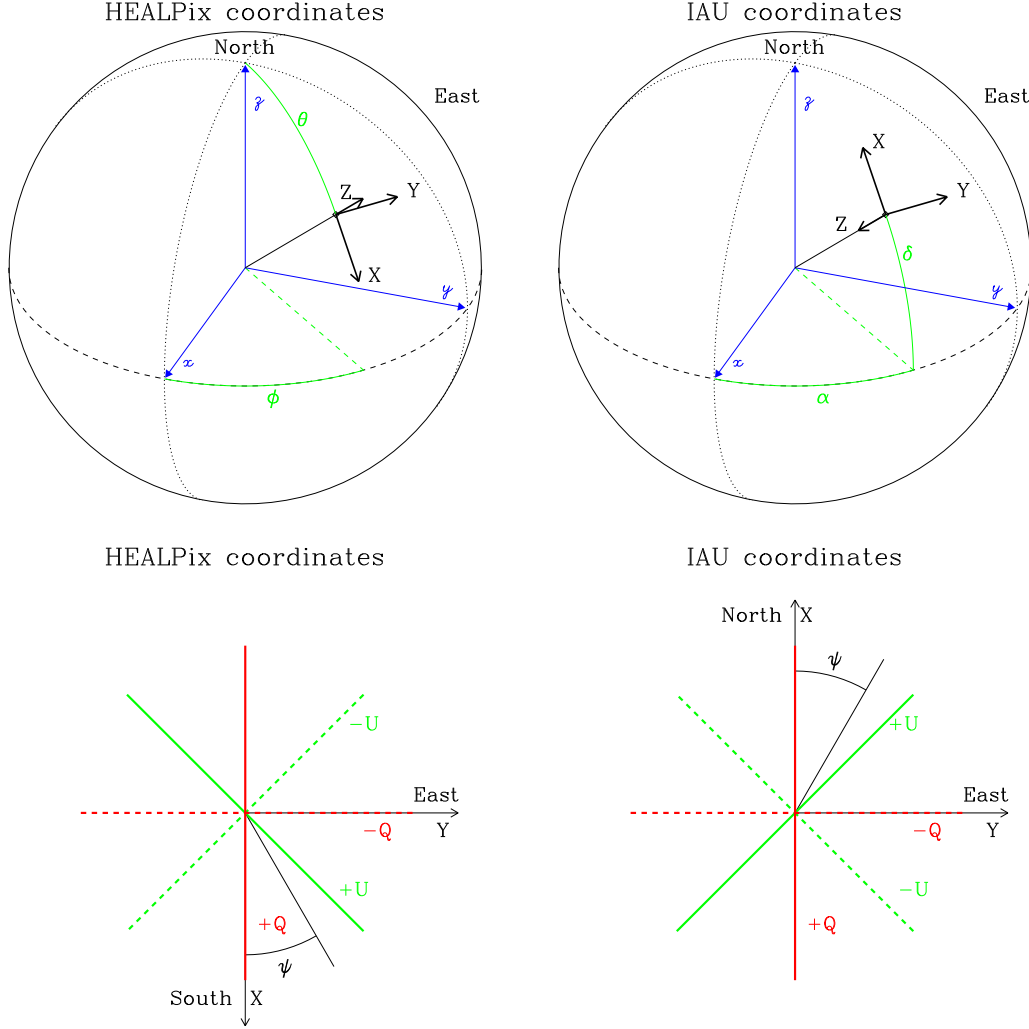
Figure 5: Coordinate conventions for **HEALPix** (*lhs* panels) and IAU (*rhs* panels). The upper panels illustrate how the spherical coordinates are measured, and the lower panel how the Q and U Stokes parameters are identified in the tangential plan.

`COSMO` for files following the Healpix/CMB/*Planck* convention (default for sky map synthetized with Healpix routine `synfast`) or `IAU` for those following the IAU convention, as defined above. Absence of this keyword is interpreted as meaning `COSMO`.

The `change_polcconv` IDL facility is provided to add this keyword or change/update its value and swap the sign of the U Stokes parameter, when applicable, in an existing FITS file.

The facility `anafast` will crash if the map to analyze follows the 'IAU' convention, and issue a warning if the convention used can not be determined.

A.4   Spherical harmonic conventions

The Spherical Harmonics are defined as

$$Y_{\ell m}(\theta, \phi) \;=\; \lambda_{\ell m}(\cos\theta)\mathrm{e}^{im\phi} \tag{21}$$

where the

$$\lambda_{\ell m}(x) \;=\; \sqrt{\frac{2\ell + 1}{4\pi}\frac{(\ell - m)!}{(\ell + m)!}}\,P_{\ell m}(x), \quad \text{for } m \geq 0 \tag{22}$$

$$\lambda_{\ell m} \;=\; (-1)^m\lambda_{\ell|m|}, \quad \text{for } m < 0,$$

$$\lambda_{\ell m} \;=\; 0, \quad \text{for } |m| > \ell.$$

Introducing $x \equiv \cos\theta$, the associated Legendre Polynomials $P_{\ell m}$ solve the differential equation

$$(1 - x^2)\frac{d^2}{dx^2}P_{\ell m} - 2x\frac{d}{dx}P_{\ell m} + \left(\ell(\ell + 1) - \frac{m^2}{1 - x^2}\right)P_{\ell m} \;=\; 0. \tag{23}$$

They are related to the ordinary Legendre Polynomials P_l by

$$P_{\ell m} \;=\; (-1)^m(1 - x^2)^{m/2}\frac{d^m}{dx^m}P_{\ell}(x), \tag{24}$$

which are given by the Rodrigues formula

$$P_{\ell}(x) \;=\; \frac{1}{2^{\ell}\ell!}\frac{d^{\ell}}{dx^{\ell}}(x^2 - 1)^{\ell}. \tag{25}$$

Note our $Y_{\ell m}$ are identical to those of (Edmonds, 1957), even though our definition of the $P_{\ell m}$ differ from his by a factor $(-1)^m$ (a.k.a. Condon-Shortley phase).

B   Pixel window functions

A pixelised signal $f(p)$ is the average within each pixel p (with surface area Ω_{pix}) of the underlying signal

$$f(p) \;=\; \int d\mathbf{u}\,w_p(\mathbf{u})f(\mathbf{u}) \tag{26}$$

where w_p is equal to $1/\Omega_{\mathrm{pix}}$ within the pixel, and equal to 0 outside, so that $\int d\mathbf{u}\,w_p(\mathbf{u}) = 1$. Eq. (1) then becomes

$$f(p) \;=\; \sum_{\ell=0}^{l_{max}}\sum_m a_{\ell m}w_{\ell m}(p), \tag{27}$$

where

$$w_{\ell m}(p) \quad = \quad \int d\mathbf{u} w_p(\mathbf{u}) Y_{\ell m}(\mathbf{u}), \tag{28}$$

is the Spherical Harmonic Transform of the pixel p.

However, complete analysis of a pixelised map with the exact $w_{\ell m}(p)$ defined above would be computationally intractable (because of azimutal variation of pixel shape over the polar caps of the **HEALPix** grid), and some simplifying asumptions have to be made. If the pixel is small compared to the signal correlation length (determined by the beam size), the exact structure of the pixel can be ignored in the subsequent analysis and we can *assume*

$$w_{\ell m}(p) = w_\ell(p) Y_{\ell m}(p) \tag{29}$$

where we introduced the m-averaged window function

$$w_\ell(p) \quad = \quad \left(\frac{4\pi}{2\ell+1} \sum_{m=-\ell}^{\ell} |w_{\ell m}(p)|^2 \right)^{1/2}, \tag{30}$$

which is independent of the pixel location on the sky.

If we assume all the pixels to be identical, the power spectrum of the pixelized map, C_ℓ^{pix}, is related to the hypothetical unpixelized one, C_ℓ^{unpix}, by

$$C_\ell^{\text{pix}} \quad = \quad w_\ell^2 C_\ell^{\text{unpix}} \tag{31}$$

where the effective pixel window function w_ℓ is defined as

$$w_\ell \quad = \quad \left(\frac{1}{N_{\text{pix}}} \sum_{p=0}^{N_{\text{pix}}-1} w_\ell^2(p) \right)^{1/2}. \tag{32}$$

This function is provided with the **HEALPix** package for $\ell \le 4N_{\text{side}}$ for each resolution parameter N_{side}.

The pixel window functions are now available for both temperature and polarization.

For $N_{\text{side}} \le 128$, those window functions are computed exactly using Eqs. (30) and (32). For $N_{\text{side}} > 128$ the calculations are too costly to be done exactly at all ℓ. The temperature windows are extrapolated from the case $N_{\text{side}} = 128$ assuming a scaling in ℓ similar to the one exhibited by the window of a tophat pixel. The polarization windows are assumed to be proportional to those for temperature, with a proportionality factor given by the exact calculation of w_ℓ at low ℓ.

Because of a change of the extrapolation scheme used, the temperature window functions provided with **HEALPix** 1.2 and higher for $N_{\text{side}} > 128$ are slighty different from those provided with **HEALPix** 1.1. For a given N_{side}, the relative difference increases almost linearly with ℓ, and is of the order of $\Delta w/w < 7\ 10^{-4}$ at $\ell = 2N_{\text{side}}$ and $\Delta w/w < 1.7\ 10^{-3}$ at $\ell = 4N_{\text{side}}$.

C   A Comment on the Random Number Generator

We provide a new random number generator (RNG) with this package, available both in Fortran90 and C++. It resides in `src/f90/mod/rngmod.f90` and `src/cxx/cxxsupport/planck_rng.h` and supersedes the previous RNG (which is still available at `src/f90/mod/ran_tools_dist.f90`).

It produces double precision real numbers x with $x \in]0, 1[$ and is based on a xor-shift method described by Marsaglia in Journal of Statistical Software 2003, vol 8 (cf. `http://www.cs.hku.hk/`). It accepts up to four different seeds simultaneously, allowing each sequence to have a theoretical period of $2^{128} - 1 \approx 3.410^{38}$. A Gaussian deviate RNG is also provided. See the respective routines documentation for details on their usage. Please note that we have not extensively tested this generator — it did not represent the main drive of this project.

References

Ansari, R., et al, 2003, *Planck parameter definition document* (DRAFT 2003-10-23), Technical Report PL-COM-IAS-SD-L2.02.005, ESA.

Baumgardner, J.R. and Frederickson, P.O., 1985, SIAM J. Numerical Analysis, Vol. 22, No. 6, p. 1107

Chandrasekhar, S. 1960, in Radiative Transfer (Dover: New York)

Crittenden, R.G., Coulson, D. & Turok, N.G., 1995, Phys.Rev. D52, 5402

Crittenden, R. and Turok, N.G., 1998, astro-ph/9806374

Driscoll, J.R. and Healy, D., 1994, Adv. in Appl. Math., Vol. 15, p.202

Edmonds, A.R., 1957, *Angular Momentum in Quantum Mechanics*, Princeton University Press

Goldberg, J. N., et al. 1967, J. Math. Phys. 8, 2155

Górski, K.M., Hivon, E., Banday, A. J., Wandelt, B. D., Hansen, F. K., Reinecke, M. & Bartelmann, M., 2005, ApJ, 622, 759, astro-ph/0409513

Hamaker, J.P. & Bregman, J.D., 1996, A&AS 117, 161

Hamaker, J.P. & Leahy, J.P., 2003, *"A study of CMB differencing polarimetry with particular reference to* Planck, ESA REPORT SCI-A/2003.312/JT

Hu, W. & White, M., 1997, NewA, 2, 323

IAU, 1974, Transactions of the IAU Vol. 15B (1973) 166

Kamionkowski, M., Kosowsky, A., Stebbins, A., 1997, Ph.Rev. D, 55, 7368 (KKS)

Mucaccia, P.F, Natoli, P. and Vittorio, N., 1998, ApJ., 488, L63

Saff, E.B. and Kuijlaars, A.B.J., 1997, The Mathematical Intelligencer, 19, #1, p.5

Seljak, U. & Zaldarriaga, M., Phys. Rev. Lett. **78**, 2054 (1997).

Szalay, A.S. and Brunner, R.J., 1998, astro-ph9812335, to appear in a special issue of the Elsevier journal "Future Generation Computer Systems"

Tegmark, M., 1996, 470, L81

Wandelt, B.D., Hivon, E. and Górski, K.M., 1998, astro-ph/9803317, in "Fundamental Parameters in Cosmology", proceedings of the XXXIIIrd Rencontres de Moriond, Trân Thanh Vân (ed.)

Zaldarriaga, M., 1998, ApJ, 503, 1

Zaldarriaga, M. & Seljak, U., Phys. Rev. D **55** 1830 (1997)